Progress In Electromagnetics Research Letters, Vol. 83, 23–28, 2019

Compact Dual-Band Substrate Integrated Waveguide Crossover with High Isolation

Sholampettai S. Karthikeyan*

Abstract—A compact dual-band substrate integrated waveguide (SIW) crossover with high isolation is proposed. Two identical slots are etched on the ground plane to achieve dual-band response and compact size. The passbands are generated below the cutoff frequency of the SIW due to the electric dipole behaviour of the slots. In-line ports are also employed to obtain good transmission and high isolation. To validate the concept, a dual-band crossover operating at 2.4 GHz and 5.4 GHz is designed, fabricated, and measured. The crossover size including in-line ports is $43.2 \times 43.2\,\text{mm}^2$, equivalent to $0.43\lambda_g \times 0.43\lambda_g$, here λ_g is the guided wavelength at the first operating frequency. The tested insertion loss and isolation at the two operating frequencies are smaller than 0.27 dB and greater than 40 dB, respectively.

1. INTRODUCTION

In recent years, the design of microwave components based on the substrate integrated waveguide (SIW) is increasing rapidly due to their compact size, high performance, and low cost. Therefore, there is a great demand for the development of compact multi-band microwave components such as filters, crossovers, and power dividers, which occupy less space and provide simultaneous operation at different frequencies [1–4]. Crossover is a commonly used device in monolithic microwave integrated circuits, which allows transmission lines to carry different signals to cross each other without mutual interferences. In recent years, substrate integrated waveguide (SIW) crossovers attract much attention due to low insertion loss, low cost, and high performances. Crossover finds major application in the design of Butler matrix for antenna array. Initially, crossovers have been designed using three-dimensional (3D) structures such as bond wires, underpasses, via-holes, and air-bridges [5–7]. These designs not only dispensed a problem in fabrication but also exhibited considerable return loss in the passband. Considering the drawbacks in 3D crossovers, the first planar microstrip crossover has been developed using a two-section cascaded branch-line structure [8], and then multi-section branchline structures have been employed to design the crossovers [9].

Several SIW crossovers with different techniques have been developed to achieve compact size, wide band, and filtering response [10–15]. In [10], an ultra-wideband crossover has been designed using microstrip-to-coplanar waveguide transition. A SIW crossover structure has been developed by composing four rectangular waveguide branches in the form of a cross [11]. In [12], an ultra-compact wideband SIW crossover has been designed employing electric and magnetic couplings simultaneously. In [13], orthogonal degenerate modes have been utilized to develop a filtering response SIW crossover. SIW to grounded coplanar waveguide transition has been used to design a wideband crossover [14]. The excitation of orthogonal modes has been employed to develop a wideband SIW crossover [15]. Although it is relatively compact, wide band and filtering response have been achieved, and multi-band characteristics of the SIW crossover are yet to be explored.

Received 30 January 2019, Accepted 14 March 2019, Scheduled 22 March 2019

* Corresponding author: Sholampettai Subramanian Karthikeyan (sskarthikeyan@nitt.edu).
The author is with the Department of Electronics and Communication Engineering, National Institute Technology Tiruchirappalli, Tamil Nadu 620015, India.

In this work, a novel SIW crossover with dual-band operation, compact size, and high isolation is presented. The working principle of the proposed SIW crossover is clearly elaborated with respect to the achieved performances. The design idea of this crossover is to utilize the electric dipole behaviour of the slots to achieve compact size and dual-band operation. In addition, in-line ports are used to obtain high isolation levels. More description would be explained in as follows.

2. DUAL-BAND CROSSOVER DESIGN

The configuration of the proposed dual-band crossover (composed of a rectangular cavity, in-line ports, and slots) is presented in Fig. 1. Two identical slots are etched on the ground plane to achieve dual-band characteristic. In-line ports are employed to achieve good transmission and isolation performances. Due to the electric dipole behaviour of slots, passbands are achieved below the cutoff frequency of the SIW. The proposed dual-band SIW crossover is developed by the following three steps. First, the dominant mode cutoff frequency of the SIW can be computed by the following equation [8]:

$$f_{c(TE10)} = \frac{c}{2W_{eff}\sqrt{\epsilon_r}} \tag{1}$$

$$W_{eff} = W - \frac{d^2}{0.95S} \tag{2}$$

where W_{eff} and W are the effective width and width of the SIW, respectively. S and d are the space between vias and the diameter of the metallic vias, respectively. ϵ_r is the relative permittivity of the substrate, and c is the velocity of light in vacuum. Secondly, two identical slots are etched on the bottom layer of the SIW to achieve dual-band operation. There are two parameters to determine passband characteristics: the length L_s of the slots and the distance of separation g between the slots. These dimensions can be optimized using full-wave simulator to obtain popular frequency bands. Finally, the in-line ports are realized to achieve good transmission and high isolation.

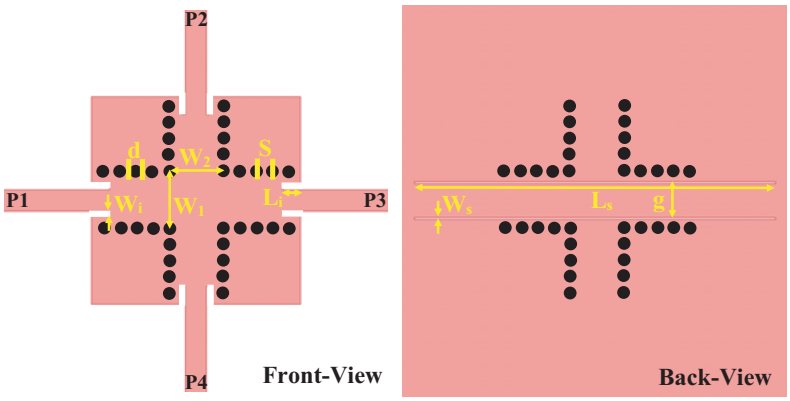

Figure 1. Schematic topology of the proposed SIW dual-band crossover.

Based on the dimensions of the proposed structure, the frequency responses are simulated and investigated. Table 1 shows the dimensions of the proposed configuration for all the design cases. Fig. 2 illustrates the magnitude responses for different lengths of the slots. Various frequency bands can be obtained by varying the length of the slots. From the plot, it is seen that the return loss and isolation are greater than 20 dB and 40 dB, respectively. Also, the insertion loss is smaller than 0.5 dB for all the examples. Similarly, the variation of the frequency bands for different values of g is presented in Fig. 3. The simulated magnitude response of S_{22} and S_{42} of the dual-band SIW crossover working at 2.4 and 5.4 GHz is depicted in Fig. 4. The length (L_s) and distance of separation (g) can be optimized to achieve popular frequency bands. Parameters W_i and L_i are chosen to provide good matching so that the maximum power can be transmitted to the output. From the simulation analysis we find that the return loss can be reduced by increasing the values of W_i and L_i. It is also found that the operating

Table 1. Dimensions of the proposed dual-band crossover (unit: mm).

Designs	W_1	W_2	S	D	L_i	W_i	L_s	W_s	g
Type A	10	10	1.2	0.6	2	0.34	25	0.3	4
Type B	10	10	1.2	0.6	2	0.34	30	0.3	4
Type C	10	10	1.2	0.6	2	0.34	35	0.3	4
Type D	10	10	1.2	0.6	2	0.34	40	0.3	4
Type x	10	10	1.2	0.6	2	0.34	40	0.3	1.5
Type y	10	10	1.2	0.6	2	0.34	40	0.3	2.5
Type z	10	10	1.2	0.6	2	0.34	40	0.3	3.5

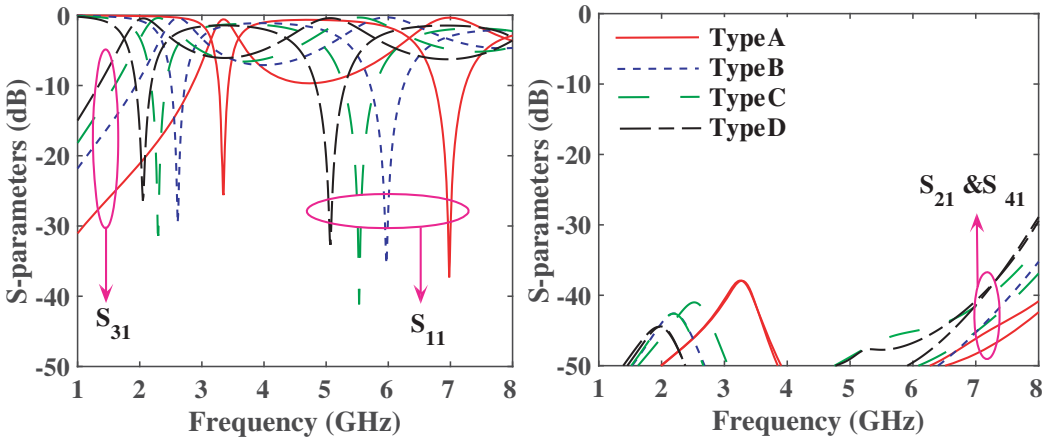

Figure 2. Simulated S-parameters for different design examples with respect to various L_s and fixed gap between two slots.

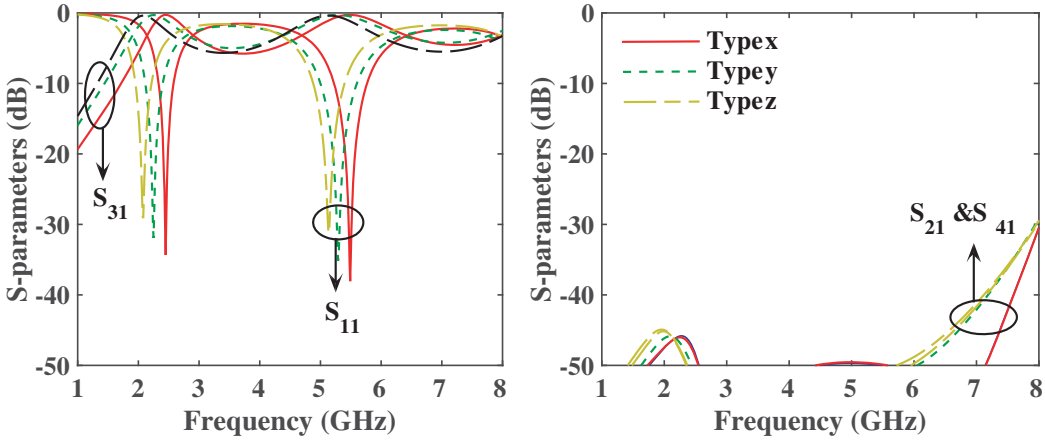

Figure 3. Simulated S-parameters for different design examples with respect to various g and fixed length of the slots.

frequencies can be shifted by varying parameter W_S. The operating frequencies could be shifted to smaller values by increasing the value of W_S. For a constant value of g, the value of L_S can be changed to obtain different operating frequencies. The value of L_S can be increased in order to achieve smaller operating frequencies, but the frequency ratio (f_2/f_1) will be the same and vice-versa.

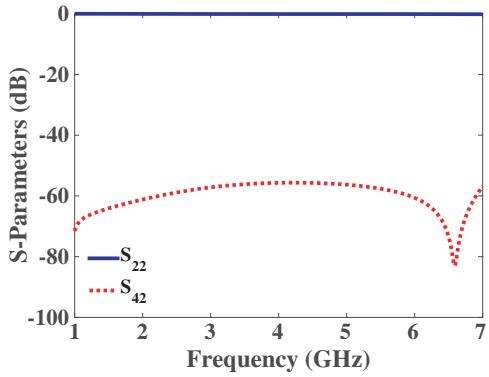

Figure 4. Simulated magnitude response of S_{22} and S_{42} of the dual-band SIW crossover working at 2.4 and 5.4 GHz.

3. FABRICATION, MEASUREMENT AND RESULTS

In order to validate the concept, a dual-band SIW crossover operating at 2.4 and 5.4 GHz is realized on a Rogers RT/duroid 5870 substrate having thickness of 0.787 mm, dielectric constant of 2.33, and loss tangent of 0.001. The optimized dimensions of the proposed dual-band SIW crossover in Fig. 1 are as follows: $W_1 = 10$ mm, $W_2 = 10$ mm, $S = 1.2$ mm, $d = 0.6$ mm, $L_i = 2$ mm, $W_i = 0.34$ mm, $L_s = 40$ mm, $W_s = 0.3$ mm, and $g = 3.6$ mm. Fig. 5 shows photographs of the fabricated prototype. The overall circuit size of the prototype including in-line ports is $0.43\lambda_g \times 0.43\lambda_g$.

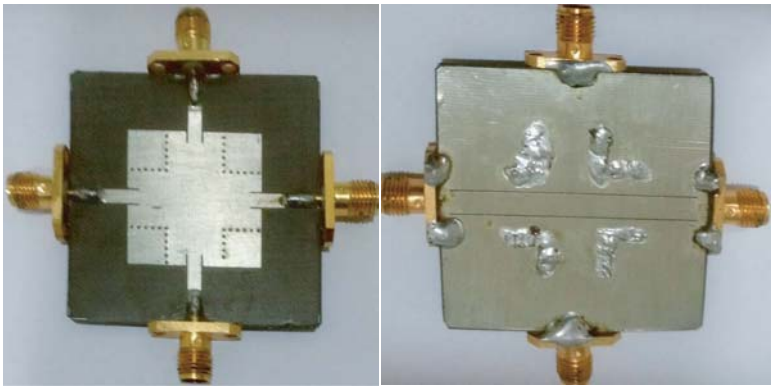

Figure 5. Photograph of the fabricated dual-band crossover.

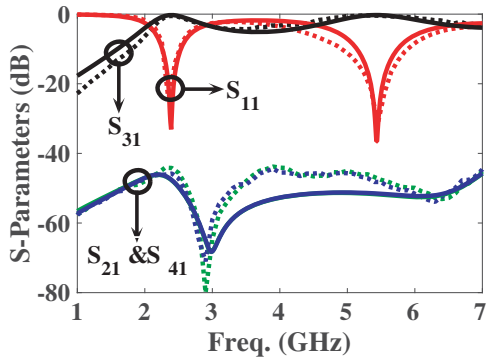

Figure 6. Simulated (solid-line) and measured (dotted-line) return loss (S_{41}) of the fabricated dual-band SIW crossover.

Table 2. Comparison between proposed and current state-of-the-art SIW crossovers (SB: Single-Band, DB: Dual-Band).

References	[11]	[12]	[13]	[14]	[15]	This Work
Operation	SB	SB	SB	SB	SB	DB
IL (dB)	0.5	0.9	1.63	< 4	0.83	< 1
RL (dB)	13	17	21	> 10	18.8	> 20
Isolation (dB)	20	17	30	> 20	20	> 40
Size (λ_g^2)	1.44	17.76	6.29	6.35	4.06	0.234

Figure 6 illustrates the comparison between simulated and measured S-parameters of the proposed dual-band SIW crossover, which are obtained by using a full-wave simulator and a Rohde & Schwarz ZVL network analyzer, respectively. The measured return loss (S_{11}) at the first passband is 21.4 dB with a 10 dB fractional bandwidth of 11.2%. The tested minimum insertion loss (S_{31}) within the first passband is 0.51 dB. At the second passband, the measured return loss (S_{11}) is 26.3 dB with a 10 dB fractional bandwidth of 10.9%. The tested minimum insertion loss (S_{31}) within the second passband is 0.27 dB. The measured isolation (S_{41}) at both the passbands is greater than 40 dB. A very small deviation is observed between simulated and tested results due to the fabrication tolerance and connector loss. Table 2 shows the comparison of the proposed dual-band SIW crossover and other reported SIW crossovers. It is clearly seen that the footprint of the proposed SIW crossover is smaller than those reported in [11–15], while it provides dual-band operation and high isolation.

4. CONCLUSION

In this paper, a novel compact dual-band SIW crossover with good isolation performance is presented. The proposed structure is composed of a rectangular cavity, in-line ports, and slots etched on the ground plane. The dual-frequency operation is achieved due to the electric dipole characteristic of the slots, and in-line ports are utilized for good transmission and isolation responses. A prototype working at 2.4 and 5.4 GHz is synthesized, fabricated, and tested. The experimental results are in good agreement with the simulated one.

REFERENCES

1. He, Z., J. Cai, Z. Shao, X. Li, and Y. Huang, "A novel power divider integrated with SIW and DGS technology," *Progress In Electromagnetics Research*, Vol. 139, 289–301, 2013.
2. Hesari S. S. and J. Bornemann, "Substrate integrated waveguide crossover formed by orthogonal TE_{102} resonators," *European Microwave Conference (EuMC)*, 17–20, 2017.
3. Zhang X. C, Z. Y. Yu, and J. Xu, "Novel band-pass Substrate Integrated Waveguide (SIW) filter based on Complementary Split Ring Resonators (CSRRs)," *Progress In Electromagnetics Research*, Vol. 72, 39–46, 2007.
4. Cassivi, Y., L. Perregrini, P. Arcioni, M. Bressan, K. Wu, and G. Conciauro, "Dispersion characteristics of substrate integrated rectangular waveguide," *IEEE Microw. Wireless Compon. Lett.*, Vol. 12, No. 9, 333–335, 2002.
5. Horng, S. T., "A rigorous study of microstrip crossovers and their possible improvements," *IEEE Trans. Microw. Theory Tech.*, Vol. 42, No. 9, 1802–1806, 1994.
6. Becksa, T. and I. Wolff, "Analysis of 3-D metallization structures by a fullwave spectral-domain technique," *IEEE Trans. Microw. Theory Tech.*, Vol. 40, No. 12, 2219–2227, 1992.
7. Yang, Y. H. and G. N. Alexopoulos, "Basic blocks for high-frequency interconnects," *IEEE Trans. Microw. Theory Tech.*, Vol. 36, No. 8, 1258–1264, 1988.
8. Wight, S. J., J. W. Chudobiak, and V. Makios, "A microstrip and stripline crossover structure," *IEEE Trans. Microw. Theory Tech.*, Vol. 24, No. 5, 270–270, 1976.

9. Yao, J., C. Lee, and P. S. Yeo, "Microstrip branch-line couplers for crossover application," *IEEE Trans. Microw. Theory Tech.*, Vol. 59, No. 1, 87–92, 2011.
10. Abbosh, A., S. Ibrahim, and M. Karim, "Ultra-wideband crossover using microstrip-to-coplanar waveguide transitions," *IEEE Microw. Wireless Compon. Lett.*, Vol. 22, No. 10, 500–502, 2012.
11. Djerafi, T. and K. Wu, "60 GHz substrate integrated waveguide crossover structure," *European Microwave Conference (EuMC)*, 1014–1017, 2009.
12. Guntupalli, A., T. Djerafi, and K. Wu, "Ultra-compact millimeter-wave substrate integrated waveguide crossover structure utilizing simultaneous electric and magnetic coupling," *IEEE/MTT-S Int. Microw. Symp. Dig.*, 1–3, 2009.
13. Han, S., K. Zhou, J. Zhang, C. Zhou, and W. Wu, "Novel substrate integrated waveguide filtering crossover using orthogonal degenerate modes," *IEEE Microw. Wireless Compon. Lett.*, Vol. 27, No. 9, 803–805, 2017.
14. Abbosh, A., S. Ibrahi, and M. Karim, "A wideband single-layer crossover using substrate integrated waveguide to grounded coplanar waveguide transition," *Microw. Opt. Technol. Lett.*, Vol. 59, No. 11, 2757–2762, 2017.
15. Zhou, Y., K. Zhou, J. Zhang, C. Zhou, and W. Wu, "Miniaturized substrate integrated waveguide filtering crossover," *IEEE Electrical Design of Advanced Packaging and Systems Symposium (EDAPS)*, 1–3, 2017.